Cell Prolif. 2002, **35** (Suppl. 1), 48–59

A continuum model to analyse spatial cell fluxes from positional labelling data applied to cell migration in oral mucosa

D. Barthel*, F. A. Meineke*, C. S. Potten†‡ and M. Loeffler*

**University of Leipzig, Institute of Medical Informatics, Statistics & Epidemiology, Liebigstrasse 27, Leipzig D-04103, Germany, †Paterson Institute for Cancer Research, Christie Hospital NHS Trust, Wilmslow Road, Manchester, M20 4BX, UK, and ‡EpiStem Limited, Incubator Building, Grafton Street, Manchester, M13 9XX, UK*

Abstract. A novel method is presented which allows the estimation of the velocity of migrating cells from positional ^{3}HTdR labelling data in spatially organized epithelial tissues. In a continuum approach, wave-like profiles of labelling index (LI) data, which travel away from the basal layer, are followed and compared with experimental LI profiles. The method yields estimates of migration velocity, cell flow, and turnover time. Results for the ventral tongue mucosa in a group of 55 BDF1 mice that were labelled at the same time of the day and culled at different time points within a 24-h period have been analysed. The results show a strong circadian rhythm in the migration velocity and the related parameters.

Keywords: cell migration, cell positional analysis, continuum model, oral mucosa.

INTRODUCTION

In the first of a series of four papers on oral mucosa Potten *et al.* (2002) investigated the cell kinetic properties of the murine ventral tongue epithelium. They observed rapid changes in the labelling index after ^{3}HTdR pulse labelling and in the mitotic activity through a 24-h period. Here we present a more detailed analysis of some of their data. Our primary interest is in the spatial organization of the tissue, in particular in the cell flux into the suprabasal cell layer from the basal cell layer. A review of the data reveals a contrast between a relatively time invariant pattern of positional cell density (many cells near the basal layer, gradually fewer at larger distance), a rapid dynamics of label travelling through the tissue and a pronounced circadian rhythm of cell division. It is our aim to obtain quantitative insight into the transition of cells from the basal cell layer to the suprabasal layers and the velocity of cell migration through the suprabasal layer. The motion of the cells cannot be observed directly. However, modelling methods can yield some quantitative information. Here we describe a novel method to estimate migration velocities from the observed positional frequencies of labelled cells followed with time after a pulse label. The methods and applications are general but will be illustrated for the murine oral mucosa dataset.

Correspondence: Dr D. Barthel, University of Leipzig, Institute of Medical Informatics, Statistics & Epidemiology. Liebigstrasse 27, Leipzig D-04103, Germany

MATERIALS AND METHODS

The experimental procedure used to investigate the oral mucosa was described by us in Potten *et al.* (2002). Briefly, 55 animals that were not influenced by irradiation or chemical substances were labelled with ^{3}HTdR at day 0 at 15.00 h. They were culled 40 min, or 2, 4, 6, 8, 12, 16 or 24 h later. Sections of the oral mucosa of the ventral tongue were prepared and investigated with the Axiohome microscope system to obtain a morphometric analysis (see Potten *et al.* 2002 for details).

Data acquisition

For each animal, five areas of observation were defined and evaluated. For each cell identified by its nucleus, the position of the nucleus in a given two-dimensional co-ordinate system, the state of labelling (labelled/nonlabelled), and the location relative to the basal cell layer (basal/nonbasal) were recorded.

Spatial cell distribution

To obtain an insight into the spatial distribution of cells an analysis was performed separately for each sectioned area. For each cell the nearest distance from the basal cell layer, x was calculated. Discrete cell positions were defined by choosing an interval of $\Delta x = 10$ μm and defining for $I = 0, 1, \ldots, 8$

$$Int_i = \{x | i \cdot \Delta x \leq x < (i + 1) \cdot \Delta x\}. \tag{1.1}$$

Using W as the width of the area under observation, we define the (empirical) cell density at position i as:

$$\rho_i = \frac{\#\text{ cells in position } i}{\Delta x \cdot W}. \tag{1.2}$$

In an analogous way the positional density of labelled cells is defined by

$$\rho l_i = \frac{\#\text{ labelled cells in position } i}{\Delta x \cdot W}, \tag{1.3}$$

and the ratio of both density functions is the positional labelling index

$$LI_i = \frac{\rho l_i}{\rho_i} = \frac{\#\text{ labelled cells in position } i}{\#\text{ cells in position } i}. \tag{1.4}$$

In a second step, the results were aggregated for all areas of animals that belong to the same treatment group, i.e. with the same time span from labelling to culling. Means, standard deviations (SD) and standard errors (SEM) were calculated. Additionally, because of only slight variations of the cell density profile over a 24-h period, a normalized profile of cell density was calculated by averaging over all areas under investigation.

The kinematic migration model

In our model, the distance x from the basal cell layer can vary continuously, so the cell density is formally defined for each value of $x \geq 0$ by

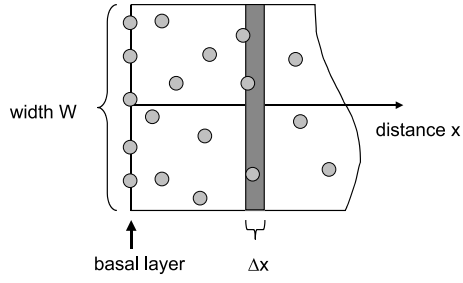

Figure 1. Sketch of a microscopic section through a polarized epithelial tissue. Vertical line at the left side: basal cell layer. *W*, width of the section; *x*, co-ordinate; position, distance from basal layer.

$$\rho(x) = \lim_{\Delta x \to 0} \frac{\#\text{ cells with position } X | x \le X < x + \Delta x}{W \cdot \Delta x}. \tag{1.5}$$

The data show an exponential decrease in the cell density ρ with increasing distance *x*. Therefore, it will be justified in this special case to consider density–distance relationships of the special type

$$\rho(x) = \rho_0 \cdot e^{-\lambda \cdot x}. \tag{1.6}$$

The motion of cells is described by a position-dependent velocity function $u(x)$. According to the measurements (see below) it is assumed that $\rho(x)$ does not change with time. Thus, it is reasonable to assume the same for $u(x)$.

The simplified geometry of a microscopic section preparation as it is realized by the model can be seen in a sketch in Fig. 1. The basal layer is a straight line of length *W*. *x* describes the position relative to the basal cell layer. The narrow shaded rectangle on the right side is a hypothetical region of points with distance *X* within the interval $x \le X < x + \Delta x$. The position of the left borderline, *x*, and the width of the rectangle, Δx, are chosen arbitrarily, but Δx is assumed to be small. Influx into and outflux from this region will now be considered. After a time span of

$$\Delta t = \frac{\Delta x}{u(x)},$$

all cells from inside the rectangle will have moved outside to the right. Their number must be the product of the cell density and the area of the rectangle, i.e.

$$\rho(x) \cdot W \cdot \Delta x = \rho(x) \cdot u(x) \cdot W \cdot \Delta t. \tag{1.7}$$

Because of the postulated time independence of the cell density, the same number of cells must have moved into this rectangle from an adjoining rectangle of the same width on the left side, i.e. from the basal cell layer side, so the flow of cells, i.e. the number of cells that move through a vertical line at position *x* related to the time span under observation per width *W* is given by

$$I = \rho(x) \cdot u(x), \tag{1.8}$$

and has the same value for all positions *x* (condition of continuity). Consequently, the velocity *u* has to change with the position *x* according to

$$u(x) = \frac{I}{\rho(x)}. \tag{1.9}$$

If the cell density decreases exponentially (equation 1.6), the velocity has to increase exponentially:

$$u(x) = u_0 \cdot e^{\lambda x} \quad \text{with} \quad u_0 = \frac{I}{\rho_0}. \tag{1.10}$$

The density of labelled cells, $\rho l(x,t)$ can be defined by analogy to the cell density. Because of the time-dependent outflow of labelled cells from the basal cell layer, the model must allow variations of $\rho l(x,t)$ with time t. The same holds for the positional labelling index

$$LI(x,t) = \frac{\rho l(x,t)}{\rho(x)}. \tag{1.11}$$

The flow of labelled cells can change with time. However, regarding the narrow rectangle mentioned above, a difference in numbers of entering and leaving labelled cells must result in an equal change in the number of labelled cells within it. Under these conditions, we derive the following partial differential equation (PDE) for the positional labelling index in a streaming tissue, which is the central model equation:

$$I \cdot \frac{\partial LI(x,t)}{\partial x} + \rho(x) \cdot \frac{\partial LI(x,t)}{\partial t} = 0. \tag{1.12}$$

This PDE can be solved analytically using the method of characteristics, which yields the general solution:

$$LI(x,t) = f\left[t - \frac{1}{I} \cdot \int_0^x \rho(x') \cdot dx' \right]. \tag{1.13}$$

where $f(\tau)$ is an arbitrary well-behaved function of τ. If the cell density $l(x)$ decreases exponentially, equation 1.13 reduces to

$$LI(x,t) = f\left[t - \frac{1}{u_0 \cdot \lambda} \cdot (1 - e^{-\lambda x}) \right]. \tag{1.14}$$

This can be interpreted by analogy to a plane wave as a profile of LI that moves in the x direction and, because of the exponential increase of the velocity, undergoes distortion.

In order to obtain a solution of the PDE that applies to a specific problem, the general solution has to be restricted by initial and boundary conditions. The initial condition states that $LI(x,t)$ at time $t = 0$ has to be identical with a given initial profile $LI_{init}(x)$:

$$LI(x,0) = LI_{init}(x), \tag{1.15}$$

whereas the boundary condition demands that $LI(x,t)$ at position $x = 0$ has to follow a given time course $LI_{border}(t)$:

$$LI(0,t) = LI_{border}(t). \tag{1.16}$$

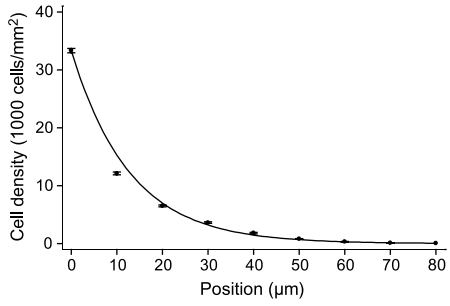

Figure 2. Cell density profile of the ventral tongue mucosa. Averaged 275 areas scored from 55 mice. Abscissa, distance from basal layer; ordinate, cell density. Error bars: measured values, mean ± SEM. Curve, exponential regression line $\rho = \rho_0 * \exp(-\lambda * x)$, parameters $\rho_0 = 33\,300 \pm 2500$ cells/mm^2, $\lambda = 0.0780 \pm 0.0057$ µm^{-1}.

Both $LI(x,t)$ and $LI_{border}(t)$ have to be estimated from observations. Obviously the function $f(\tau)$ has to be chosen as

$$f(\tau) = LI_{border}(\tau). \tag{1.17}$$

An explicit calculation of $LI(x, t)$ can use the analytical solution (1.17) thus avoiding numerical solving methods.

Estimation of the model parameters

The measured values of the positional cell density can be used to specify the function $\rho(x)$.

As was mentioned above, a plot of empirical values indicates that the positional cell density decreases exponentially with distance from the basal layer (Fig. 2), so equation 1.6 is an appropriate model equation with two parameters ρ_0 (cell density at position 0) and λ (logarithmic decrement) that can be estimated by nonlinear regression. Consequently, the migration velocity increases exponentially (equation 1.10). The value of the parameter u_0, however, cannot be derived in this way.

Provided that the kinematic model describes the movement and distortion of LI profiles in an appropriate way and given a provisional value of u_0 (e.g. by making a guess), it is possible to predict the shape of a LI profile at a time point t_{end} if the shape at an earlier time point t_{begin} is known. Actually, LI profiles were measured at times $t_j = 0, 2, 4, 6, 8, 12, 16, 24$ h ($j = 0, 1, \ldots, 7$) for discrete positions x_i, so it is possible for all time intervals $[t_j, t_{j+1}]$ ($j \le 6$) to use the experimental profile at time $t_{beg} = t_j$ as a starting profile from which a theoretical profile at time $t_{end} = t_{j+1}$ can be calculated. The latter can be compared with the experimental profile at the same time t_{j+1}. The degree of coincidence depends on the provisional value of u_0. A good guess should produce similar profiles. To make this fitting concept work, one has to define a measure of difference between observed and theoretical profiles. Following Press *et al.* (1992), one calculates the weighted sum of the squared differences between observed LI values and the corresponding model values. One has to sum up over all observed positions x_i and to use the reciprocal squared errors of the observed LI values as weight. (The method will be demonstrated with actual data in the Results section.) Therefore, by defining a measure X^2 according to

$$X^2 = \sum_{k=1}^{n} \frac{[li_k(\text{model}) - li_k(\text{observed})]^2}{\text{var}(li_k)}, \tag{1.18}$$

and using a minimization algorithm, a value of u_0 that makes X^2 minimal can be found. This value is an estimate of the mean migration velocity at position 0 during the time interval $[t_j, t_{j+1}]$. We used the Levenberg–Marquardt algorithm, which is implemented in the program system Mathcad 2001. Therefore, repeating this procedure for all $j = 0, 1, \ldots, 6$ the velocity at position 0, u_0 and the flow $I = \rho_0 \cdot u_0$ can be estimated for all time spans between neighboured time points of observation.

RESULTS

Profile of the cell density

As Fig. 2 shows, the cell density profile in the oral mucosa can be described by an exponential distribution (equation 1.17). Using the method of nonlinear regression with the empirical variance of ρ_i values as a weight function, the estimated values of the distribution parameters were $\rho_0 = 33\,300 \pm 2500$ cells/mm^2, $\lambda = 0.0780 \pm 0.0057$ µm^{-1}. ρ_0 is in accordance with the directly observed empirical cell density of $32\,450 \pm 720$ cells/mm^2 in the 10 µm-interval adjoining position 0. As a consequence of equation 1.17, the local cell density at the position

$$x_h = \frac{\ln 2}{\lambda} \tag{2.1}$$

is only 50% of the density at position 0, i.e.

$$\rho(x_h) = \frac{1}{2} \cdot \rho_0, \tag{2.2}$$

and the logarithmic decrement λ can be replaced by the more transparent half-value depth x_h with a value of 8.89 ± 0.65 µm. Furthermore, the fraction of all cells which are located between positions 0 and an arbitrarily chosen $x_{\max}$ is

$$p(x_{\max}) = \frac{\int_0^{x_{\max}} \rho(x) \cdot dx}{\int_0^{\infty} \rho(x) \cdot dx} = (1 - e^{-\lambda \cdot x_{\max}}) = 1 - \left(\frac{1}{2}\right)^{\frac{x_{\max}}{x_h}}, \tag{2.3}$$

which means that 50% of all cells are between positions 0 and x_h, but 98.4% between 0 and $6 \cdot x_h = 53.4 \pm 3.9$ µm. This is in accordance with the observed average thickness of 51.1 ± 1.1 µm.

Profiles of the labelling index

The observed sequence of LI-profiles at increasing time intervals after pulse labelling is shown in Fig. 3a and the corresponding set of time courses at different positions in Fig. 3b. These graphs are derived from the data presented in Potten *et al.* (2002), Fig. 1.

Circadian variation of cell migration (velocity u_0) from the basal to the suprabasal cell layer

For each of the six time intervals between two consecutive measurements, an estimate of u_0 was calculated by minimizing the distance measure X^2. In Fig. 4, the method is demonstrated for the first time span (0–2 h after labelling). The resulting values of u_0 are given in Table 1, column

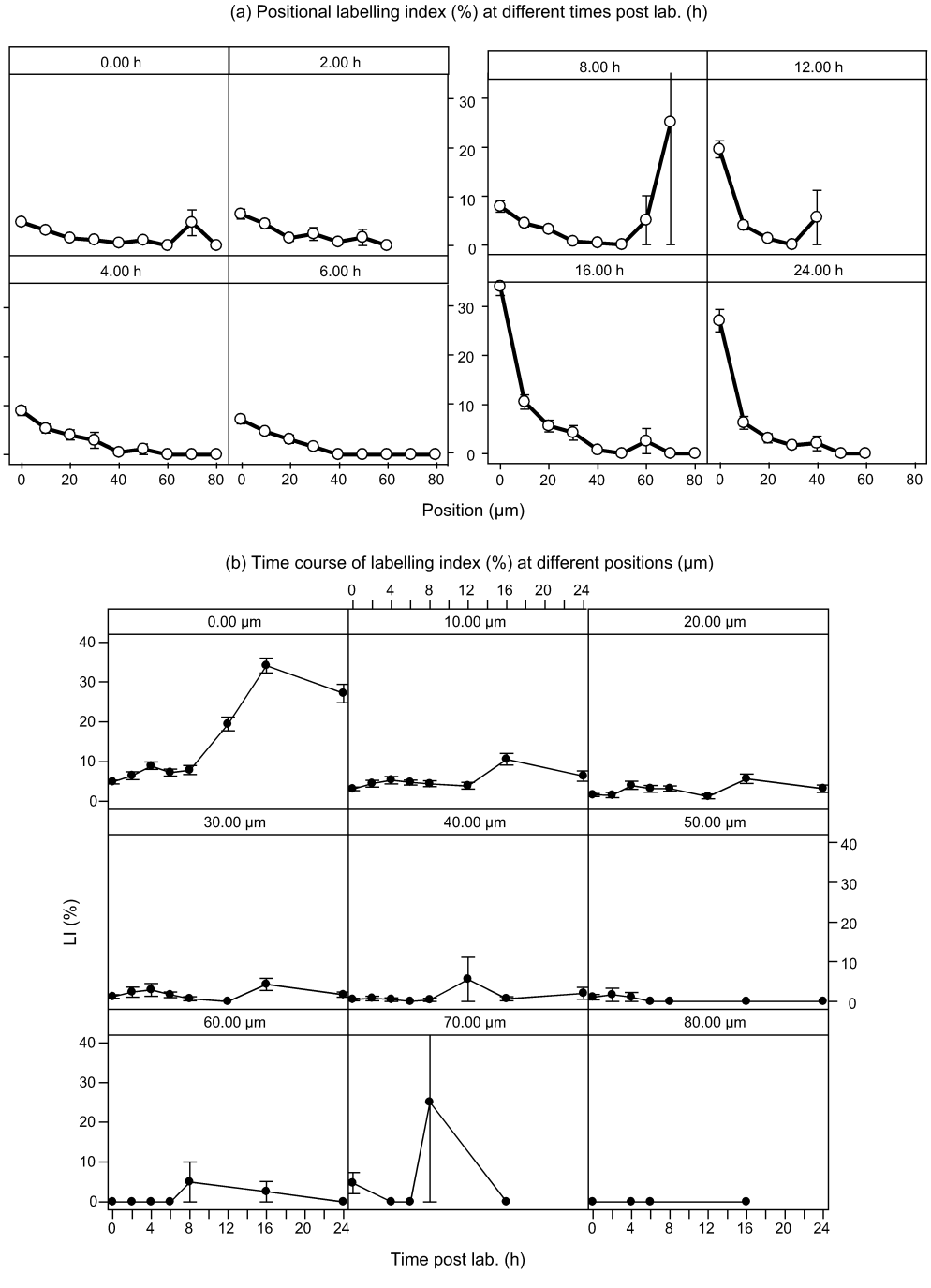

Figure 3. (a) LI profiles vs. position at different times after labelling. mean ± SEM. Panel strips: time, h. (b) Time course of LI at different positions, mean ± SEM. Panel strips: position, µm.

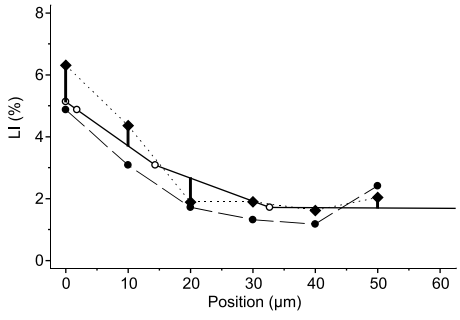

Figure 4. Demonstration of the method of fitting parameter u_0. The experimental LI profile (closed circles, connected by the broken line, measured at the start time t_{beg}) is the same as in Figure 3a, left panel in the first row. Assuming a starting value of u_0, a shift and distortion of this profile can be calculated. Each closed circle shifts to the right (●) or disappears beyond the right border and a model profile under the assumption of a specific choice of u_0 is constructed (○, connected by the full line). The observed profile at time t_{end}, which is the same as in Figure 3a, right panel in the first row, is represented by (◆) connected by dotted lines. The fitting procedure searches a value u_0 that minimizes the distance measure between the theoretical (model) profile and the observed profile at t_{end} (thick vertical bar).

Table 1. Estimates of migration velocity u_0, the cell flow I, and the cell production rate r for different time intervals after labelling and averaging

I	From	To	u_0 (µm/h)	I (cells/mm/h)	r (%/h)
0	15.00	17.00	0.85	28.2	12.7
1	17.00	19.00	1.06	35.5	15.9
2	19.00	21.00	0	0	0
3	21.00	23.00	0.03	0.9	0.4
4	23.00	03.00	0	0	0
5	03.00	07.00	0.56	18.7	8.4
6	07.00	15.00	0	0	0
Mean			0.26	8.5	3.8

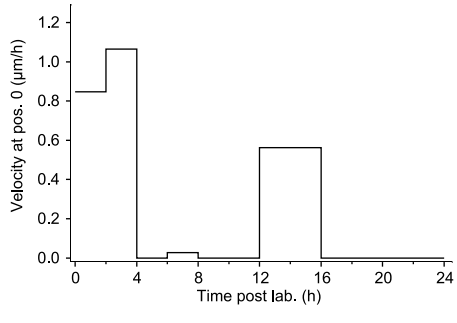

Figure 5. Estimated migration between the basal and suprabasal cell layer over one day (velocity parameter u_0). Abscissa, time after labelling; ordinate, value of u_0.

4. Figure 5 summarizes the results for the estimates of the cell flux leaving the basal cell layer and entering the suprabasal cell layer. We identify two activity peaks over 24 h.

From the velocity parameter u_0, two other parameters of biological interest can be derived (Table 1, columns 5 and 6). One is the cell flow $I = \rho_0 \cdot u_0$ according to equation 1.10. The second is the rate of cell production (movement from the basal layer) which is given by

$$r = \frac{\#\text{ cells outflowing from basal line}/(W \cdot \Delta t)}{\#\text{ cells in basal line}/(W \cdot \Delta t)} = \frac{1}{\#\text{ cells in basal line}/W}. \tag{2.4}$$

Furthermore the number of basal cells per top line width W can be estimated to 222.5 ± 2.9 cells/mm.

Mean migration velocities

If one is interested only in parameter values which are averaged over the whole 24-h period, one has to take the different lengths $\Delta t(i)$ into account by calculating weighted means, so the mean velocity at position 0 can be calculated accordingly to be

$$\bar{u}_0 = \frac{\sum_1^7 u_0(i) \cdot \Delta t(i)}{\sum_1^7 \Delta t(i)}, \tag{2.5}$$

resulting in a value of

$$\bar{u}_0 = 0.255\ \mu\text{m/h}.$$

Calculating the mean flow in the same way leads to $\bar{I} = 8.5$ cells/(mm · h). The mean cell production rate resulting is $\bar{r} = 3.8\%/\text{h}$. From the latter a mean transit time of

$$\bar{T} = \frac{1}{\bar{r}} = 26.2\ \text{h}$$

through the suprabasal cell layer is deduced.

Estimating wave fronts

By using the model and the estimated individual values of u_0, one can follow up the positions of distinct fronts of the LI. Within the time intervals and a constant value of u_0, a front with the initial position x_{beg} at time t_{beg} moves according to

$$x(t) = x_{beg} + \frac{1}{\lambda} \cdot \ln \frac{1}{1 - u_0 \cdot \lambda \cdot e^{\lambda \cdot x_{beg}} \cdot (t - t_{beg})}. \tag{2.6}$$

For a period of a whole day or several days, the movement within each subinterval has to be matched. In Fig. 6 this is was done for a period of two days for fronts starting from positions of 0, 2, … , 18, and 20 μm, respectively. As can be seen, a cell starting from the basal cell layer (position $x_{beg} = 0$) leaves the system after 48.7 h while cells starting from suprabasal positions, such as 10 or 20 μm, leave the suprabasal layer already after 15.6 or 2.9 h. Hence this estimate implies a surprisingly short time interval that cells survive if they are placed at high positions

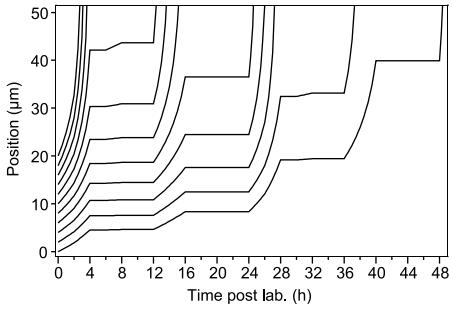

Figure 6. Change of position during cell migration. Abscissa, time after labelling; ordinate, distance from basal cell layer. The curves show the movement of cells away from the basal layer dependent on their starting position at time 0.

in the suprabasal layer. Figure 6 also illustrates that the mean transit time for cells entering the suprabasal cell layer at the bottom (position 0) to reach the top (position 50) is about 50 h. About 1 day will be spent on travelling from position 0 to position 10, while 1 day is needed to reach the top positions from here. The major reason for this acceleration of cell migration is the continuous increase of the mean cell sizes and the accompanying decline of (nuclear) cell density.

DISCUSSION

The model described in this paper was developed because of the need for quantitative information on the spatial migration of cells in spatially organized polar tissues, which cannot be observed directly. The method uses positional index data obtained at various (narrowly spaced) time intervals after a pulse label. Furthermore, it needs data on the spatial cell density along the axis of cell migration. Because of the large number of positional data obtained for oral mucosa (see Potten *et al.* 2002) a continuum approach could be chosen. Zajicek and his coworkers (Zajicek 1986, 1995; Zajicek & Arber 1991) have modelled polarized tissues as regions of streaming fluids. A direct connection between their work and our investigations, however, does not exist, so, to our best knowledge, no comparable attempt to estimate the velocity of migration has been made.

We applied the method to analyse cell migration in the oral mucosa. A special mechanical property of the oral mucosa is the position-dependent cell density. According to the actual data, we restricted ourselves to simple exponentially decreasing functions. As equation 1.13 shows, more general types of density profiles described by monotonically decreasing functions are compatible with the framework of the model. Because of the continuity equation, a local decrease in the density is always accompanied with a local increase in the velocity. It should be noted that the analogy with the mechanics of streaming fluids is incomplete because here no attempt was made to introduce mechanical forces. Therefore, the model is purely kinematic, not dynamic. Nevertheless, given the positional distribution of cells as an empirical fact, it is possible to derive consequences for the velocity.

A crucial point is the assumption that all, or at least most, of the suprabasal cells have a nucleus so that all cells remain visible in the microscopic section provided that their nucleus is situated in the plane of cutting. An alternative assumption could be that the cells gradually lose

their nuclei as they migrate so that they become invisible but continue to exist. As a consequence, the observed exponential decrease in nuclear density according to equation 1.6 is the result of loss of nuclei in the cells according to kinetics of first order, namely

$$\frac{d\rho}{dt} = k \cdot \rho$$
$$\rho = \rho_0 \cdot e^{-k \cdot t} \tag{3.1}$$

with a rate constant k and a half-value time of

$$t_{\frac{1}{2}} = \frac{\ln 2}{k}. \tag{3.2}$$

Because at the same time the cells move in the x-direction with a uniform velocity u, the logarithmic decrement λ depends on the rate constant k and the velocity u according to

$$\lambda = \frac{k}{u}. \tag{3.3}$$

Furthermore, in contrast to equation 1.14 the positional index $LI(x,t)$ now has the general form

$$LI(x,t) = f(t - \frac{x}{u}) \tag{3.4}$$

where $f(\tau)$ is an arbitrary function of τ. Therefore, all points of the LI profile move with the same velocity u so that the form of the profile remains unchanged.

If one speculates that the cells move over a distance of 50 μm in 50 h and $\lambda = 0.078\ \mu m^{-1}$ as before, the migration velocity is $u = 1.0$ μm/h at all cell positions x, the rate constant is $k = 0.078\ h^{-1}$, and the half-value time is $t_{1/2} = 8.9$ h. This would mean that 50% of the cells which have migrated over a distance of 8.9 μm have lost their nucleus. Actually, we cannot believe that the observed decrease in nuclear density over a range of several orders of magnitude is only because the cells have become invisible. It cannot be excluded, however, that cell acceleration and nuclear loss take place in parallel. It remains unclear how to quantify their relative importance.

The analysis of the oral mucosa suggests that there are two periods of migration activity, i.e. a rapid migration at 15.00–19.00 h, a moderate migration at 05.00–09.00 h and no migration in the interim intervals. A comparison with the results of Potten *et al.* (2002, Figs 2 and 3) shows concordance with the times of maximal basal labelling index, which fall into the periods mentioned above, whereas the single maximum of the mitotic index falls into the first period.

Similar circadian-dependent variations in cell migration have been reported for the gastrointestinal system (Qiu *et al*. 1994). However, the method of these workers failed when we tried to proceed in this way with the oral mucosa data. The reason was probably the strong decrease in the cell density in the oral mucosa in contrast to the approximately position-independent cell density in the crypt.

We also tried to estimate the basal cell production rate and basal cell turnover time with a method that we developed for the investigation of changes in the murine epidermis after a mechanical stimulus (Potten *et al.* 2000). In this two-compartment approach, the steepness of

the time course of the normalized number of labelled cells in the combined basal–suprabasal compartment is a measure of the cell production rate in the basal layer. This is correct under the assumption that cell divisions occur only in the basal layer and that the number of labelled cells increases only by division of labelled cells. The data, which were the same as above, yielded a cell production rate of $r = 13.6\%/\text{h}$ and a turnover time of

$$T = \frac{1}{r} = 7.3 \text{ hours}$$

with the unrealistic consequence of three successive cell cycles within one day. Potten *et al.* (2002) came to the same result when they observed an amplification in the basal labelling index within 24 h by a factor of approximately $8 = 2^3$. This was interpreted as a delayed uptake of ^{3}HTdR from a long-term intracellular thymidine pool. The model presented here can effectively adjust for such overlaying effects. For each time interval, the start profile is treated as an external input into the model and the end profile is regarded as a reference dataset.

In an independent approach Potten *et al.* (2002) derived from their data on vincristine accumulation a basal turnover rate of 54%/day, which is equivalent to a turnover time of 44.4 h, so at the moment, the estimates of the turnover time are scattered over a fairly wide range. The model which is presented in this paper uses positional information not as an artefact but as reality.

A major biological finding of this analysis is the increasing cell migration velocity through the suprabasal layer. This is directly related to the increase in cell sizes. Biologically this implies that well-organized and rapid processes must exist to integrate the cell remnants into the epithelium surface. Furthermore, minor perturbances of the cell size development may grossly effect the epithelial organization.

REFERENCES

Potten CS, Barthel D, Li YQ, Ohlrich R, Matthe B, Loeffler M (2000) Proliferation in murine epidermis after minor mechanical stimulation. Part 1. Sustained increase in keratinocyte production and migration. *Cell Prolif* **33**, 231–246.

Potten CS, Booth D, Cragg NJ, Tudor GL, O'Shea JA, Appleton D, Barthel D, Gerike TG, Meineke FA, Loeffler M, Booth C (2002) Cell kinetic studies in the murine ventral tongue epithelium. thymidine metabolism studies and circadian rhythm determination. *Cell Prolif* **35** (Suppl. 1) 1–15.

Press WH, Teukolsky SA, Vetterling WT, Flannery BP (1992) *Numerical Recipes in C: the Art of Scientific Computing*, 2nd edn. Cambridge: Cambridge University Press, 681–688.

Qiu JM, Roberts SA, Potten CS (1994) Cell migration in the small and large bowel shows a strong circadian rhythm. *Epithelial Cell Biol*. **3**, 137–148.

Zajicek G (1986) The application of kinematic equations for the Study of cell turnover. *J. Theor. Biol*. **120**, 141–149.

Zajicek G, Arber N (1991) Streaming kidney. *Cell Prolif*. **24**, 375–382.

Zajicek G (1995) Streaming organism. *Med. Hypotheses* **45**, 403–407.